CrystEngComm

Accepted Manuscript

This is an *Accepted Manuscript*, which has been through the Royal Society of Chemistry peer review process and has been accepted for publication.

Accepted Manuscripts are published online shortly after acceptance, before technical editing, formatting and proof reading. Using this free service, authors can make their results available to the community, in citable form, before we publish the edited article. We will replace this *Accepted Manuscript* with the edited and formatted *Advance Article* as soon as it is available.

You can find more information about *Accepted Manuscripts* in the Information for Authors.

Please note that technical editing may introduce minor changes to the text and/or graphics, which may alter content. The journal's standard Terms & Conditions and the Ethical guidelines still apply. In no event shall the Royal Society of Chemistry be held responsible for any errors or omissions in this *Accepted Manuscript* or any consequences arising from the use of any information it contains.

ROYAL SOCIETY OF CHEMISTRY

www.rsc.org/crystengcomm

CrystEngComm RSCPublishing

PAPER

Synthesis of three-dimensional AlN-Si_3N_4 branched heterostructures and their photoluminescence properties †

Cite this: DOI: 10.1039/x0xx00000x

Received 00th June 2014
Accepted 00th XXX 2014

DOI: 10.1039/x0xx00000x

www.rsc.org/crystengcomm

J. Cai,[a] Y. L. Zhang,[a] Y. Li,[a] L.Y. Du,[a] Z.Y. Lyu,[a] Q. Wu,[a] X. Z. Wang*[a] and Z. Hu[a]

Synthesis of heterostructures with branched morphology is of great importance for exploiting novel physical and chemical properties in nanoscience and nanotechnology field. In this study, combining with the extended vapor-liquid-solid (EVLS) and vapor-solid (VS) growth methods, we successfully fabricate three-dimensional (3D) AlN-Si_3N_4 branched heterostructures with the core of Si_3N_4 nanostructures and branched AlN nanocones with the adjustable diameter and length. The photoluminescence (PL) spectra of the AlN-Si_3N_4 branched heterostructures display the new emission bands besides that of the as-synthesized Si_3N_4 nanostructures, which may be ascribed to the emission bands of AlN in the deep- or trap-level state. These results propose a general strategy for designing and preparing 3D branched heterostructures for novel optoelectronic devices.

Introduction

Heterostructures have attracted great attentions due to their unique optical, electronic, magnetic and chemical properties derived from the interactions of the junctions, and promising applications in solar cells[1, 2], photoelectric devices[3, 4], Li ion batteries[5-7], etc. To date, a variety of functional heterostructures with axial, radial and branched morphology have been fabricated[8-12]. For example, the hierarchical ZnO arrays on NiO nanowires can improve the photon adsorption of pure ZnO [13]. The ZnO-ZnSe heterostructures extend the absorption of the pure ZnO from ultraviolet region to the visible region[14]. CuO nanostructures on ZnO nanowires have potential applications by means of maximizing junction areas and active sites[15]. The lattice matched ZnTe shell on CdSe nanowires can obtain the improving photovoltaic performance owing to inhibiting interfacial recombination of photon-generated carrier[16].

As well-known, Si_3N_4 (5.3 eV) and AlN (6.2 eV) are important wide band gap semiconductors and ceramic materials owing to their excellent mechanical strength, remarkable thermal stability, modulated electrical and optical properties by doping and morphology control[17, 18]. Up to now, one-dimensional (1D) nanostructures of single Si_3N_4 and AlN, including nanowires, nanobelts, nanotubes, and nanocones, have been synthesized and their optoelectronic properties have been explored[18-24]. In our previous reports, Si_3N_4 nanobelts were prepared by using the Fe-Si alloy particles as 'catalyst' based on the extended vapor-liquid-solid (EVLS) growth mechanism[22]. AlN nanocones arrays were synthesized on silicon wafer using $AlCl_3$ vapor and gaseous NH_3 as Al and N source, which exhibited good field emission properties[18].

Herein, we report the novel three-dimensional (3D) AlN-Si_3N_4 branched heterostructures with the adjustable diameter and length of AlN nanocones on Si_3N_4 nanowires prepared by combination with the EVLS and vapor-solid (VS) growth methods. Photoluminescence (PL) measurements show that AlN-Si_3N_4 heterostructures display the new emission bands besides that of the as-synthesized Si_3N_4 nanostructures. This result provides a general strategy for designing and preparing functionalization heterostructures.

Experimental

Synthesis of one-dimensional (1D) Si_3N_4 nanostructures. Synthesis of 1D Si_3N_4 nanostructures is similar to our previous report[22]. The micron-sized Fe-Si alloy particles were used as 'catalyst' for growing Si_3N_4 1D nanostructures based on the extended vapor-liquid-solid (EVLS) growth mechanism. In a typical procedure, these 'catalyst' particles were spread on an alumina wafer and then placed at the centre of a horizontal tubular furnace. The chamber was repeatedly vacuumed by rotary pump and filled with Ar to remove O_2 and moisture, and then heated to 1350 °C in N_2 flow of 50 sccm (standard cubic centimetre per minute) for 15 h. Subsequently, the system was spontaneously cooled down to ambient temperature in 50 sccm N_2 flow.

Synthesis of three-dimensional (3D) AlN-Si_3N_4 heterostructures. Synthesis of 3D AlN-Si_3N_4 branched heterostructures was carried out in a two-zone horizontal tubular furnace as shown in Fig. 1. In a typical run, the as-synthesized 1D Si_3N_4 nanostructures were located at the centre of the reaction zone, and $AlCl_3$ powders were placed at the centre of sublimation zone. The chamber was repeatedly vacuumed by rotary pump and filled with Ar to remove O_2 and moisture. Subsequently，under the Ar flow of 200 sccm, the sublimation zone and the reaction zone were simultaneously

CrystEngComm Accepted Manuscript

heated to 140 °C and 650 °C, respectively. Then NH_3 flow of 20 sccm was added into the system and reacted with the gaseous $AlCl_3$ in the reaction zone for 10, 30, 60, and 120 min. Finally, the furnace was spontaneously cooled down to ambient temperature in Ar flow of 20 sccm.

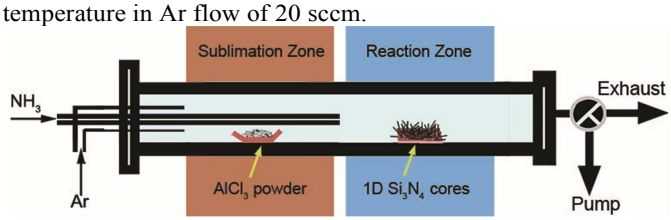

Fig.1 Schematic diagram of reaction system.

Characterizations. The morphology, structure, and chemical component of the as-prepared products were characterized by scanning electron microscopy (SEM, Hitachi S-4800) attached with an energy-dispersive X-ray spectroscopy (EDS, Ametek, EDAX-Genesis-XM2-Imaging-60SEM), high resolution transmission electron microscope (HRTEM, JEOL, JEM-2100, operating at 200 kV), and X-ray diffraction (XRD, Bruker X-ray diffractometer, D8 Advance A25, Co target, λ_{Ka1}=1.78897 Å, Fe filter of 0.02 mm thickness) with a step size of 0.02044 ° and scan speed of 0.6 s/step. Raman measurements were carried out in LabRAM ARAMIS (Horiba Jobin Yvon, 532 nm wavelength laser). The photoluminescence (PL) spectra were obtained through FLS-920 using the 325 nm line of a He–Cd laser as the excitation source.

Results and discussion

From XRD patterns shown in Fig. 2 and Fig. S1 (Supporting Information SI-1), the diffraction peaks of as-synthesized Si_3N_4 product are indexed as *h*-Si_3N_4 (α, β) and *c*-FeSi (ε). After chemical vapor deposition of AlN, new weak diffraction peaks assigned to *h*-AlN appear. With elongating the deposition time, the intensity peaks of *h*-AlN become stronger, indicating the formation of more and more *h*-AlN phase. The signal of NH_4Cl comes from the undecomposed residue during the cooling process. Furthermore, the Raman measurements in Fig. S2 (Supporting Information SI-2) indicate that two Raman shifts at 608 and 651 cm^{-1} occur in all AlN-containing samples, which are assigned to the A1 (TO) and E2 phonon modes of *h*-AlN (space group P63mc)[18]. Namely, the AlN-Si_3N_4 heterostructures are successfully synthesized.

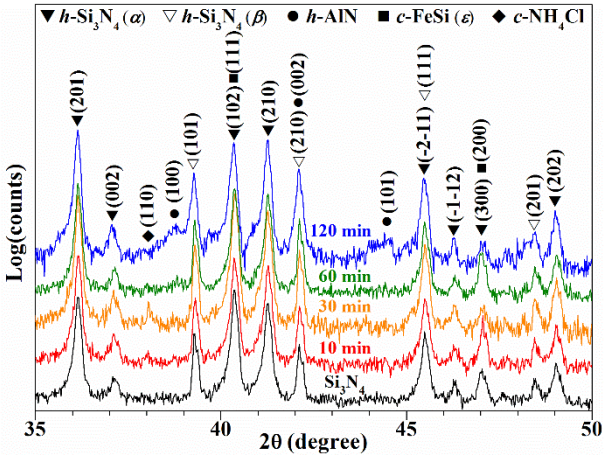

Fig. 2 XRD patterns of as-synthesized Si_3N_4 and AlN-Si_3N_4 heterostructures. The peaks marked with a triangle (▼), hollow triangle (▽) solid circle (●), and solid square (■), corresponding to *h*-Si_3N_4 (α, PDF#83-0700), *h*-Si_3N_4 (β, PDF#76-0453), *h*-AlN (PDF#75-1620), *c*-FeSi (ε, PDF#88-1298) and *c*-NH_4Cl (PDF#73-0365). Deposition times for AlN are 10, 30, 60, and 120 min.

The morphology and structures of the as-synthesized 1D Si_3N_4 nanostructures are shown in Fig. 3. It can be clearly seen that there are many nanowires grown out of the Fe-Si alloy after nitridation at 1350 °C, which have tens to hundreds of nanometers in diameter and tens to hundreds of microns in length (Fig. 3a, b). Fig 3c is the typical TEM image of a nanowire with ca. 80 nm in diameter. The corresponding HRTEM image in Fig. 3d displays the interplanar spacings of 3.9 and 2.8 Å, corresponding to the d_{110} and d_{002} of *h*-Si_3N_4 (α), respectively.

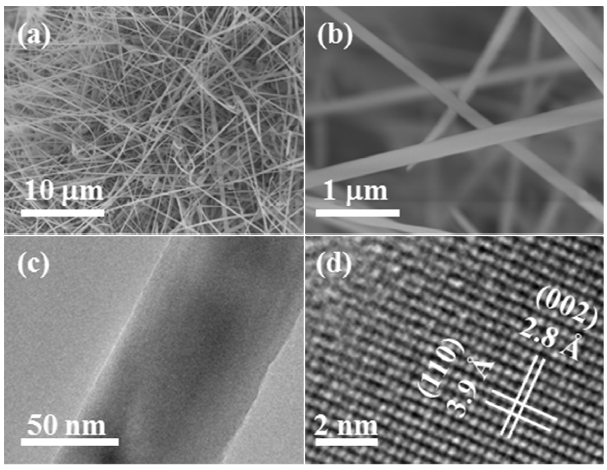

Fig. 3 The morphology and structures of 1D Si_3N_4 nanostructures synthesized at 1350 °C. (a-d) Typical SEM, TEM, and HRTEM images. The interplanar spacings of 3.9 Å and 2.8 Å corresponded to d_{110} and d_{002} of *h*-Si_3N_4(α).

After deposition of AlN at 650 °C for 30 min on the as-synthesized Si_3N_4 nanostructures, the typical morphology of 3D branched heterostructures are clearly seen in Fig. 4, presented by the different magnifications of SEM images. Many nanocones with diameters of 10-20 nm and length of several hundred nanometers grow out of the surface of as-synthesized Si_3N_4 nanostructures.

CrystEngComm Accepted Manuscript

This journal is © The Royal Society of Chemistry 2014

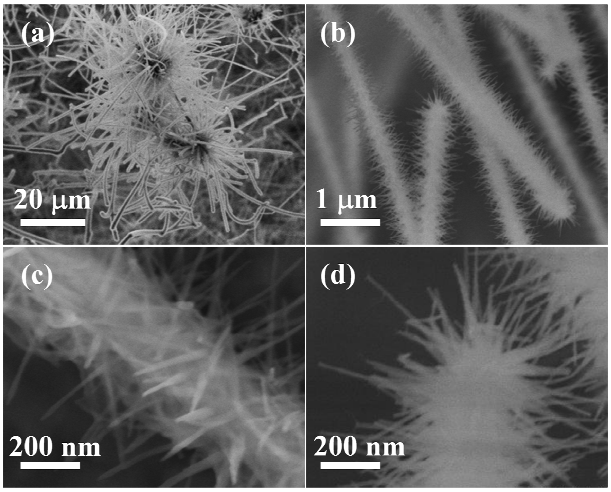

Fig. 4 Typical SEM images with different magnifications after the growth of AlN nanocones on the surface of 1D Si_3N_4 nanostructures.

Furthermore, typical elemental mapping images of Si, Al, and N from a single 3D branched heterostructure are shown in Fig. 5. The profiles of Al (Fig. 5c) and N (Fig. 5d) elements are almost the same as the morphology of the single heterostructure (Fig. 5a) while the profile of Si element (Fig. 5b) is obviously narrow. This indicates that the core of 3D branched heterostructures is composed of Si and N elements and the shell of nanocones consists of Al and N elements. Namely, AlN nanocones are deposited on the surface of 1D Si_3N_4 nanostructures to form 3D AlN-Si_3N_4 branched heterostructures.

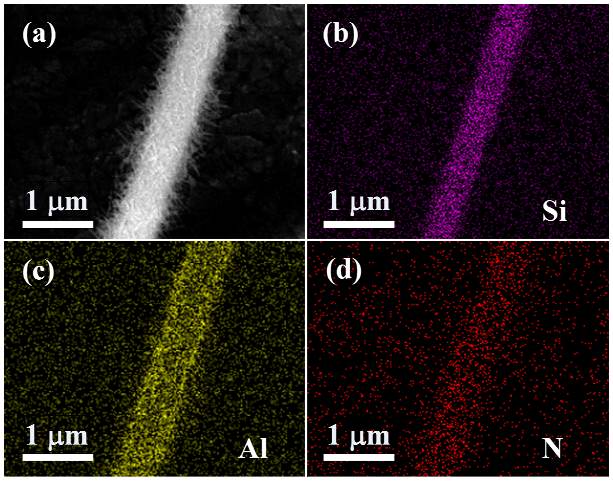

Fig. 5 Typical SEM image (a) of a single 3D branched AlN-Si_3N_4 heterostructures and corresponding elemental mapping images of Si (b), Al (c), and N (d) from EDS.

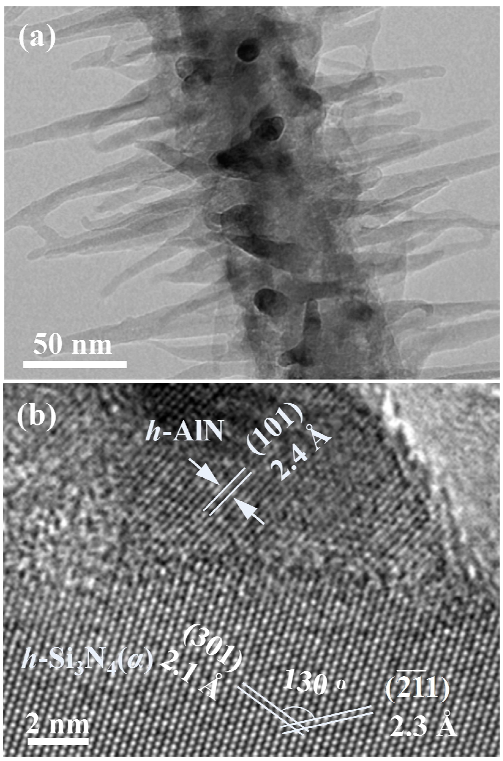

Fig.6 Typical TEM (a) and HRTEM (b) images of 3D AlN-Si_3N_4 branched heterostructures.

To investigate the microstructures of 3D AlN-Si_3N_4 branched heterostructures, TEM and HRTEM observations were carried out as shown in Fig. 6 and Fig. S3 (Supporting Information SI-3). TEM image in Fig.6a indicates that the nanocones are less than 20 nm in diameter, in consistent with the SEM observations in Fig. 4. A typical HRTEM image in Fig. 6b clearly displays that nanocones with the interplanar spacing of 2.4 Å corresponding to d_{101} of *h*-AlN and the core with the interplanar spacings of 2.3 and 2.1 Å with dihedral angle of 130 ° assigned to $d_{\bar{2}11}$ and d_{301} of *h*-Si_3N_4 (α), which is consistent with the results of elemental mappings in Fig. 5. From Fig. 6b, the lattice fringes show an abrupt change between *h*-Si_3N_4 nanostructure and *h*-AlN nanocone, i.e. the interface between Si_3N_4 and AlN is sharp. There are few diffused interface between Si_3N_4 and AlN because, at 650 °C, Al should be difficult to diffuse into Si_3N_4 surface layer with high melting point of 1900 °C.

The above-mentioned results, including XRD, Raman, SEM, EDS, and HRTEM, clearly reveal that the 3D AlN-Si_3N_4 branched heterostructures are successfully synthesized, whose core and shell are Si_3N_4 nanowire and AlN nanocones, respectively. The corresponding evolutions of the growth process is proposed as the scheme shown in Fig. 7. Firstly, 1D Si_3N_4 nanostructures are grown from micron-sized Fe-Si alloy particles in N_2 flow at 1350 °C followed the EVLS growth mechanism[22]. Specifically, the Fe-Si alloy particles firstly melt into the liquid state at 1350 °C. After the introduction of N_2 gas, N_2 molecules are dissociated to N atoms on the surface of the liquid Fe-Si alloy 'catalyst', and then N atoms diffuse into the Fe-Si liquid droplet and react with the Si atoms of liquid Fe-Si alloy to form Si_3N_4 species. After the concentration of Si_3N_4 species in the liquid droplet are supersaturated, Si_3N_4 species nucleate on the surface of the liquid Fe-Si alloy and epitaxially grow into 1D Si_3N_4 nanostructures along the direction of the minimum interface energy

CrystEngComm Accepted Manuscript

between the liquid and solid interface. Subsequently, with the introduction of $AlCl_3$ vapor and gaseous NH_3 as Al and N source, AlN is firstly nucleated on the surface of Si_3N_4 nanostrucures (as core, Fig. S4 in Supporting Information SI-4) and then grown gradually into nanocones (as shell) based on VS growth mechanism[18]. The longer the deposition time is, the thicker and longer AlN nanocones grow (Fig. 7, Fig. S5 in Supporting Information SI-5). Finally, 3D AlN-Si_3N_4 branched heterostructures with the adjustable diameter and length of AlN nanocones are formed.

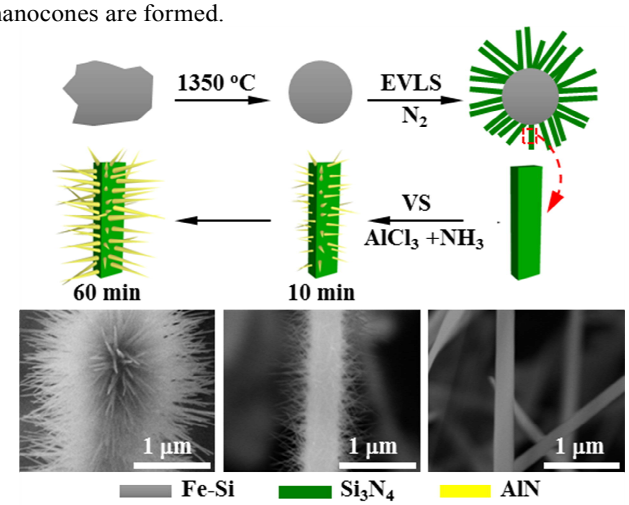

Fig. 7 Schematic evolutions from 1D Si_3N_4 nanostructures to 3D AlN-Si_3N_4 branched heterostructures.

The optical properties are investigated by PL technique with excitation length of 325 nm at low temperature (10 K). The typical PL spectrum of the as-synthesized 1D Si_3N_4 nanostructures in Fig. 8 shows near ultraviolet (UV)-visible luminescence bands located in the wavelength range of 350 and 500 nm. They can be ascribed to the defect energy levels in the Si_3N_4 nanostructures, such as those of Si-Si, N-N, ≡Si and =N[25-28]. After depositing the shell of AlN nanocones on the core of 1D Si_3N_4 nanostructures, the new emission bands occurs compared to the as-synthesized Si_3N_4 nanostructures, which can be assigned to the deep- or trap-level state of AlN such as O impurities and Al vacancy complex with one negative charge[18, 29]. This further indicates the formation of AlN nanocones around Si_3N_4 nanostructures.

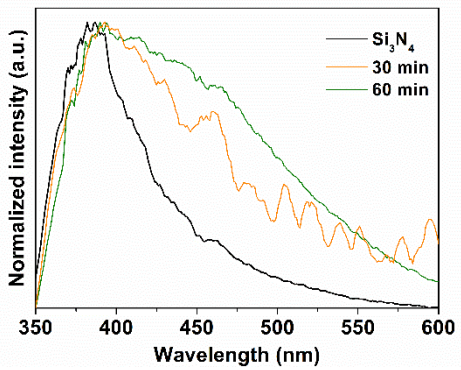

Fig. 8 PL spectra of as-synthesized 1D Si_3N_4 nanostructures and 3D AlN-Si_3N_4 branched heterostructures. The PL spectra were measured with excitation length of 325 nm at low temperature (10 K). Deposition times for AlN are 0, 30, and 60 min.

Conclusions

In summary, the 3D AlN-Si_3N_4 branched heterostructures have been synthesized in combination with firstly nitrifying micron-sized Fe-Si alloy particles through EVLS growth method and then depositing AlN nanocones via VS growth method. The data from XRD analysis, Raman measurements, SEM observations, EDS and HRTEM characterizations clearly reveal that the branched heterostructures consist of the core of 1D Si_3N_4 nanostructures and the shell of AlN nanocones with the adjustable diameter and length. The PL spectra of the 3D AlN-Si_3N_4 branched heterostructures display the new emission bands besides that of the as-synthesized Si_3N_4 nanostructures, which may be ascribed to the emission bands of AlN in the deep- or trap-level state. These results propose a general method to design and fabricate 3D branched semiconducting heterostructures for novel optoelectronic applications.

Acknowledgements

We acknowledge the joint financial support by NSFC (21073085, 21173114, 21173115, 51232003) and the "973" program (2013CB932902).

Notes and references

* To whom correspondence should be addressed. Tel.: +86-25-83593696. E-mail:wangxzh@nju.edu.cn

[a] Key Laboratory of Mesoscopic Chemistry of MOE, School of Chemistry and Chemical Engineering, Nanjing University, Nanjing 210093, P. R. China

† Electronic Supplementary Information (ESI) available: [details of any supplementary information available should be included here]. See DOI: 10.1039/b000000x/

1 L. J. Lauhon, M. S. Gudiksen, D. Wang and C. M. Lieber, *Nature*, 2002, **420**, 57-61.
2 Y. Tak, S. J. Hong, J. S. Lee and K. Yong, *J. Mater. Chem.*, 2009, **19**, 5945-5951.
3 O. Hayden, A. B. Greytak and D. C. Bell, *Adv. Mater.*, 2005, **17**, 701-704.
4 C. Gutsche, A. Lysov, D. Braam, I. Regolin, G. Keller, Z.A. Li, M. Geller, M. Spasova, W. Prost and F.J. Tegude, *Adv. Funct. Mater.*, 2012, **22**, 929-936.
5 L. Su, Y. Jing and Z. Zhou, *Nanoscale*, 2011, **3**, 3967-3983.
6 L. Gao, H. Hu, G. Li, Q. Zhu and Y. Yu, *Nanoscale*, 2014, **6**, 6463-6467.
7 Z. Sun, W. Ai, J. Liu, X. Qi, Y. Wang, J. Zhu, H. Zhang and T. Yu, *Nanoscale*, 2014, **6**, 6563-6568.
8 A. Kargar, K. Sun, Y. Jing, C. Choi, H. Jeong, Y. Zhou, K. Madsen, P. Naughton, S. Jin, G. Y. Jung and D. Wang, *Nano Lett.*, 2013, **13**, 3017-3022.
9 M. Paladugu, J. Zou, G. J. Auchterlonie, Y. N. Guo, Y. Kim, H. J. Joyce, Q. Gao, H. H. Tan and C. Jagadish, *Appl. Phys. Lett.*, 2007, **91**,133115.
10 M. Paladugu, J. Zou, Y. N. Guo, G. J. Auchterlonie, H. J. Joyce, Q. Gao, H. H. Tan, C. Jagadish and Y. Kim, *Small*, 2007, **3**, 1873-1877.
11 A. Dong, R. Tang and W. E. Buhro, *J. Am. Chem. Soc.*, 2007, **129**, 12254-12262.
12 B. Wang, X. Jin and Z. Ouyang, *Crystengcomm*, 2012, **14**, 6888-6903.

CrystEngComm Accepted Manuscript

This journal is © The Royal Society of Chemistry 2014

13 T. Guo, Y. Luo, Y. Zhang, Y. H. Lin and C.W. Nan, *Cryst. Growth Des.*, 2014, dx.doi.org/10.1021/cg500031t.
14 W. Chen, N. Zhang, M. Zhang, X. Zhang, H. Gao and J. Wen, *Crystengcomm*, 2014, **16**, 1201-1206.
15 S. Kim, Y. Lee, A. Gu, C. You, K. Oh, S. Lee and Y. Im, *J. Phys. Chem. C*, 2014, **118**, 7377−7385.
16 K. Wang, S. C. Rai, J. Marmon, J. Chen, K. Yao, S. Wozny, B. Cao, Y. Yan, Y. Zhang and W. Zhou, *Nanoscale*, 2014, **6**, 3679-3685.
17 J. Huang, Z. Huang, S. Yi, Y. g. Liu, M. Fang and S. Zhang, *Sci. Rep.*, 2013, **3**, 3504.
18 C. Liu, Z. Hu, Q. Wu, X. Wang, Y. Chen, H. Sang, J. Zhu, S. Deng and N. Xu, *J. Am. Chem. Soc.*, 2005, **127**, 1318-1322.
19 Q. Wu, Z. Hu, X. Wang, Y. Lu, K. Huo, S. Deng, N. Xu, B. Shen, R. Zhang and Y. Chen, *J. Mater. Chem.*, 2003, **13**, 2024-2027.
20 L. W. Lin and Y. H. He, *Crystengcomm*, 2012, **14**, 3250-3256.
21 J. Huang, S. Zhang, Z. Huang, Y. Wen, M. Fang and Y. Liu, *Crystengcomm*, 2012, **14**, 7301-7305.
22 K. Huo, Y. Ma, Y. Hu, J. Fu, B. Lu, Y. Lu, Z. Hu and Y. Chen, *Nanotechnol.*, 2005, **16**, 2282-2287.
23 Q. Wu, Z. Hu, X. Z. Wang, Y. N. Lu, X. Chen, H. Xu and Y. Chen, *J. Am. Chem. Soc.*, 2003, **125**, 10176-10177.
24 W. Lei, D. Liu, P. Zhu, Q. Wang, G. Liang, J. Hao, X. Chen, Q. Cui and G. Zou, *J. Phys. Chem. C*, 2008, **112**, 13353-13358.
25 J. Robertson and M. J. Powell, *Appl. Phys. Lett.*, 1984, **44**, 415-417.
26 J. Robertson, *Philos. Mag. B*, 1991, **63**, 47-77.
27 C. M. Mo, L. D. Zhang, C. Y. Xie and T. Wang, *J. Appl. Phys.*, 1993, **73**, 5185-5188.
28 S. V. Deshpande, E. Gulari, S. W. Brown and S. C. Rand, *J. Appl. Phys.*, 1995, **77**, 6534-6541.
29 A. Sedhain, N. Nepal, M. L. Nakarmi, T. M. Al tahtamouni, J. Y. Lin, H. X. Jiang, Z. Gu and J. H. Edgar, *Appl. Phys. Lett.*, 2003, **93**, 041905.

CrystEngComm Accepted Manuscript